SGK1 activation exacerbates diet-induced obesity, metabolic syndrome and hypertension

Sierra-Ramos, Catalina ; Velazquez-Garcia, Silvia ; Vastola-Mascolo, Arianna ; Hernández, Guadalberto ; Faresse, Nourdine ; Alvarez de la Rosa, Diego

Abstract: The serum- and glucocorticoid-induced kinase 1 (SGK1) is a transcriptional target of steroid hormones including glucocorticoids or aldosterone in addition to other stimuli such as glucose. SGK1 is activated via phosphoinositide 3-kinase, placing it downstream of insulin signaling. SGK1 participates in the up-regulation of kidney Na+ reabsorption by aldosterone and has been linked to obesity-related hypertension in humans. We hypothesized that a systemic increase in SGK1 activity may trigger a multiplicity of mechanisms leading to simultaneous development of the main conditions that characterize the metabolic syndrome (MetS), including hypertension. We used a transgenic mouse model made with a bacterial artificial chromosome containing the whole mouse Sgk1 gene modified to introduce an activating point mutation. Wild type or transgenic fourteen-week old male mice were fed with standard chow diet or high-fat diet for up to 18 weeks. Development of the main features of MetS and hepatic steatosis were monitored, and in vitro adipocyte differentiation was studied. Our results show that transgenic animals under high-fat diet rapidly and markedly develop MetS characterized by obesity, glucose intolerance, insulin resistance, dyslipidemia and hypertension. In addition, SGK1 gain-of-function accelerates the development of hepatic steatosis. Our study suggests that inappropriate SGK1 activity represents a risk factor in developing MetS with hypertension and related end organ damage. Our data supports SGK1 as a possible therapeutic target in MetS and related complications and provides a useful gain-of-function model for pre-clinical drug testing.

DOI: https://doi.org/10.1530/joe-19-0275

Accepted Manuscript published as JOE-19-0275.R1. Accepted for publication: 10-Oct-2019

SGK1 activation exacerbates diet-induced obesity, metabolic syndrome and hypertension

Catalina Sierra-Ramos[1,*], Silvia Velázquez-García[1,*], Arianna Vastola-Mascolo[1], Guadalberto Hernández[1], Nourdine Faresse[2,#], Diego Alvarez de la Rosa[1]

[1]Department of Basic Medical Sciences, Institute of Biomedical Technologies and Center for Biomedical Research of the Canary Islands (CIBICAN), Universidad de La Laguna, Tenerife, Spain; [2]Institute of Anatomy, University of Zurich, Switzerland.

**These authors contributed equally to this work.*

[#]*Present address*: DIVA Expertise, 1 Place Pierre Potier, 31100 Toulouse.

Correspondence: Dr. Diego Alvarez de la Rosa, Departamento de Ciencias Médicas Básicas, Universidad de La Laguna, 38071 La Laguna, Spain. Telephone: +34-922-319-968. Fax: +34-922-319-397. E-mail: diego.alvarez@ull.edu.es.

Running head: SGK1 and metabolic syndrome development.

Keywords: insulin resistance, blood pressure, serum and glucocorticoid-induced kinase, mouse model, fatty liver.

Word count: 4587 words (excluding references and figure legends)

Abstract

The serum- and glucocorticoid-induced kinase 1 (SGK1) is a transcriptional target of steroid hormones including glucocorticoids or aldosterone in addition to other stimuli such as glucose. SGK1 is activated via phosphoinositide 3-kinase, placing it downstream of insulin signaling. SGK1 participates in the up-regulation of kidney Na^+ reabsorption by aldosterone and has been linked to obesity-related hypertension in humans. We hypothesized that a systemic increase in SGK1 activity may trigger a multiplicity of mechanisms leading to simultaneous development of the main conditions that characterize the metabolic syndrome (MetS), including hypertension. We used a transgenic mouse model made with a bacterial artificial chromosome containing the whole mouse *Sgk1* gene modified to introduce an activating point mutation. Wild type or transgenic fourteen-week old male mice were fed with standard chow diet or high-fat diet for up to 18 weeks. Development of the main features of MetS and hepatic steatosis were monitored, and in vitro adipocyte differentiation was studied. Our results show that transgenic animals under high-fat diet rapidly and markedly develop MetS characterized by obesity, glucose intolerance, insulin resistance, dyslipidemia and hypertension. In addition, SGK1 gain-of-function accelerates the development of hepatic steatosis. Our study suggests that inappropriate SGK1 activity represents a risk factor in developing MetS with hypertension and related end organ damage. Our data supports SGK1 as a possible therapeutic target in MetS and related complications and provides a useful gain-of-function model for pre-clinical drug testing.

Accepted Manuscript published as JOE-19-0275.R1. Accepted for publication: 10-Oct-2019

INTRODUCTION

SGK1 is a ubiquitously expressed AGC kinase initially characterized in rat mammary tumor cells as an immediate early gene induced by serum and glucocorticoids (Webster, et al. 1993). Its expression is also upregulated by aldosterone (Chen, et al. 1999; Naray-Fejes-Toth, et al. 1999) and other factors including glucose (Lang, et al. 2006). Once synthesized, SGK1 is activated by insulin and several growth factors through phosphoinositide 3-kinase, PDK1 and mTORC2 (Garcia-Martinez and Alessi 2008). Genetic and pharmacological approaches revealed that SGK1 participates in numerous physiological and pathophysiological processes. Excess activation of SGK1 triggers pro-fibrotic and pro-inflammatory processes (Artunc and Lang 2014). SGK1 phosphorylates signaling molecules such as GSK3β and promotes cell survival and proliferation by phosphorylating the FOXO family of transcription factors (Brunet, et al. 2001). SGK1 has an important role enhancing transepithelial Na^+ reabsorption (Chen et al. 1999; Naray-Fejes-Toth et al. 1999; Wulff, et al. 2002) and controlling blood pressure (Norlander, et al. 2017; Pearce 2003; Verrey, et al. 2003). SGK1 knockout mice have normal blood pressure, but are protected against salt-dependent hypertension in the context of a high-fat diet (Huang, et al. 2006b). In addition, SGK1 polymorphisms associate to increased blood pressure in humans (Busjahn, et al. 2002), making carriers more susceptible to blood pressure increase associated to hyperinsulinemia (von Wowern, et al. 2005). Recent studies show that SGK1 regulates adipocyte differentiation and is expressed in white adipose tissue (Di Pietro, et al. 2010). The importance of SGK1 in metabolism is further supported by studies showing that an SGK1 inhibitor reduces blood pressure and body weight in hyperinsulinemic mice (Ackermann, et al. 2011) and counteracts obesity and hyperglycemia in *db/db* mice (Li, et al. 2016). Finally, *Sgk1* polymorphisms in humans (E8CC/CT;I6CC) associate with obesity (Dieter, et al. 2004) and diabetes (Schwab, et al. 2008). In summary, multiple lines of evidence point to the serum and glucocorticoid-regulated kinase 1 (SGK1) as a common pathway impacting the development of cardiovascular risk factors such as metabolic disturbances and hypertension.

To date, the effects of excess SGK1 activity on hypertension, obesity and glucose homeostasis has not been studied. To test whether excess SGK1 activity synergically activates pathways leading to

hypertension and metabolic alterations, we took advantage of the gain-of-function transgenic *Sgk1* mouse model (Tg.sgk1) previously developed in our laboratory (Andres-Mateos, et al. 2013; Miranda, et al. 2013) in combination with the high-fat diet (HFD)-induced model of obesity and glucose intolerance. Our results demonstrated exacerbated body weight gain due to fat accumulation, adipocyte hypertrophy, dyslipidemia and hyperinsulinemia, prominent glucose and insulin intolerance and a rapid development of hypertension and fatty liver.

Accepted Manuscript published as JOE-19-0275.R1. Accepted for publication: 10-Oct-2019

MATERIAL AND METHODS

Mouse model with constitutively active SGK1 expression

Experimental procedures involving mice were approved by the University of La Laguna Ethics Committee on Research and Animal Welfare (permit no. CEIBA2016-0197) and were performed in accordance with Spanish and European Union regulations (RD53/2013 and 2010/63/EU, respectively). Generation of transgenic mice expressing a constitutively active mutant of SGK1 (Tg.*sgk1*) under its own promoter has been previously described (Andres-Mateos et al. 2013; Miranda et al. 2013). Briefly, a bacterial artificial chromosome (BAC) containing 180 kbp of mouse genomic DNA that includes the full *Sgk1* gene but no other known or predicted genes was obtained from the BACPAC Resources Center (Children's Hospital Oakland Research Institute, Oakland, CA). The BAC was modified by homologous recombination in *E. coli* to introduce point mutation S422D, which renders the kinase constitutively active (Kobayashi and Cohen 1999). The purified BAC insert was used for pronuclear injection of (C57BL/6J × SJL/J) F2 embryos. Founder animals harboring the transgene were backcrossed with C57BL/6 mice for nine generations to produce the B6.Tg.sgk1 line. Mice homozygous for the transgene were obtained by crossing heterozygous animals.

Animal procedures

Mice were kept in a 14-hour light/10-hour dark cycle at 22°C with *ad libitum* access to food and water. Mice were fed a standard chow diet (SCD; Teklad Global Rodent Diet 2014S; 2.9 kcal/g, 13% calories from fat; 4% fat, 66% carbohydrates, and 14.3% proteins). Twelve-week-old male mice were fed either SCD or high-fat diet (HFD; Research Diets 12492; 5.24 kcal/g, 60% calories from fat; 34.9% fat, 26.3% carbohydrate, 26.2% protein) for the time indicated in each experiment. Food intake and body weight (BW) were measured weekly in mice housed in grouped cages. To study body composition mice were fasted 3 hours, anesthetized by intraperitoneal injection of ketamine (37.5 mg/kg) combined with medetomidine (0.5 mg/kg) and examined by dual-energy X-ray absorptiometry (DEXA; Lunar PIXImus apparatus, GE Medical Systems); anesthesia was reverted with atipamezole (1 mg/kg). Glucose tolerance tests (GTT) were performed on animals fasted overnight and injected intraperitoneally with a glucose

bolus (2 g/kg BW). Glycemia was measured before (t=0) and 5, 15, 30, 45, 60, 90 and 120 min after injection on blood samples obtained by tail massage using a commercial glucometer (OneTouch Ultra, Johnson & Johnson). Insulin tolerance tests (ITT) were performed on unfasted mice. Insulin was injected intraperitoneally (0,75 U/kg BW) and blood glucose measurements were performed as in GTT. Insulinemia was measured using a commercial mouse ELISA Kit (Mercodia). Insulin resistance was assessed using the homeostasis model assessment (HOMA-IR) (Muniyappa, et al. 2008). Insulin sensitivity was assessed by the quantitative insulin sensitivity check index (QUICKI) (Bowe, et al. 2014; Pacini, et al. 2013). Systolic blood pressure (SBP) was measured in trained conscious mice by tail-cuff plethysmography (LE5007, Panlab Harvard Apparatus) using SeDaCom 2.0 software. Measurements were collected for three consecutive days after five days of training. SBP was measured at 20 min intervals for 1 h between 10 and 11 a.m. Mice were euthanized by cervical dislocation.

Plasma and liver biochemistry

At the time of death, blood samples were collected by cardiac puncture in 1.5 ml tubes with 150 µl 5mM EDTA or heparin (in the case of cholesterol determinations) and plasma was obtained by centrifugation. Samples were assayed for total insulin (ultrasensitive mouse insulin ELISA Kit, Mercodia), total, HDL and LDL/VLDL cholesterol (cholesterol assay kit, Abcam), triglycerides (triglyceride quantification kit, Abcam), glucose and FFA (FFA quantification Kit, Abcam). Liver triglycerides content was measured using a commercial kit (Abcam).

Tissue sampling and histology

At sacrifice, fat depots and liver were dissected and weighed. Organs were frozen in liquid nitrogen and stored at −80°C for molecular analysis or fixed by immersion in 4% formaldehyde, paraffin-embedded and processed for histology. Microtome 5 µm-thick sections were stained with hematoxylin-eosin reagent. Sections were coded for unbiased examination. Liver steatosis was evaluated using a semiquantitative scale adapted from previously validated procedures (Kleiner, et al. 2005). To that end, images from three different fields in each section were collected at 20x magnification and assigned a

Accepted Manuscript published as JOE-19-0275.R1. Accepted for publication: 10-Oct-2019

value in a four-point scale (0, no intracellular lipid drops detected; 1, 2 and 3, progressively increased abundance of lipid drops; Fig. 4).

Gene expression analysis

Total RNA was extracted from tissues or cells using a commercial kit that includes in-column DNA digestion (Total RNA spin plus, REAL, Valencia, Spain) and quantified using a Nanodrop 1000 (ThermoFischer Scientific). Relative mRNA abundance was assessed by quantitative RT-PCR (qPCR) using the comparative C_t method with RPL13A mRNA expression as normalizer. Optimal annealing temperatures and efficiency was determined for each primer pair. Primers used in this study are listed in Table 1.

Western Blot

Protein extracts were obtained from frozen tissue or cells and quantified using the bicinchoninic acid procedure (Sigma). Equal amounts of protein were resolved on SDS-PAGE (10% Mini-PROTEAN® TGX Stain-Free™ Gels, Biorad) and transferred to polyvinylidene difluoride membranes (Trans-Blot® Turbo™ Mini PVDF Transfer Packs Biorad). Western blot analysis was performed as previously described (Andres-Mateos et al. 2013) using the antibodies listed in Table 2. Signals were acquired with luminesce detector (ChemiDoc™ Touch Imaging System, Biorad) and quantified using software provided by the manufacturer.

In vitro pre-adipocyte differentiation

Vascular stromal cell fraction from WT or Tg.sgk1 mice was prepared from pooled fat pads (inguinal, axillar, epididymal and perirenal) and cultured as described (Desarzens and Faresse 2016). Cells were allowed to reach confluence and the differentiation process was initiated using DMEM supplemented with 10% fetal bovine serum (FBS) 500 µM 3-isobutyl-1-methylxanthine, 1 µg/ml insulin, 250 nM dexamethasone and 2 µM rosiglitazone for 2 days. Cells were then grown in DMEM supplemented with 10% FBS, 1 µg/ml insulin for an additional 2 days. Experiments were performed once the cells were fully differentiated (around day 20) and clear lipid droplets were observed. For determination of lipid content, cells were fixed in 4% paraformaldehyde in PBS, washed twice with water and once with 60%

isopropanol, and stained with Oil-Red-O. After excess Oil-Red-O removal and washes with water, the stained cells were permeabilized with 100% isopropanol and 10% SDS and Oil-Red-O in the eluate was measured by spectrophotometry at 520 nm.

Glucose and FFA uptake

Undifferentiated and differentiated adipocytes from WT and B6.Tg.sgk1 mouse were cultured for 24 h without serum. Cells were washed with Krebs-Ringer buffer containing 12 mM HEPES and 0.1% BSA (KRH-BSA) and then treated with 100 nM insulin for 30 min. Glucose uptake was initiated by addition of 1µCi/well of [^{3}H]-deoxy-D-glucose. After 5 min incubation cells were washed 3 times with ice-cold KRH-BSA. FFA uptake was initiated by addition of 1µCi/well of [1-^{14}C]-palmitic acid for 5 minutes and stopped by washing cells 3 times with ice-cold KRH-BSA. In both cases, cells were then lysed with 0.1 M NaOH and radioactivity was measured by scintillation counting. In parallel, protein concentration in each sample was measured using the Bradford method.

Statistical analysis

Data are reported as average ± SE. Statistical analysis was performed with Prism 7 software (Graphpad). Statistical tests used for analysis are specified in each figure legend.

Accepted Manuscript published as JOE-19-0275.R1. Accepted for publication: 10-Oct-2019

RESULTS

Constitutively active SGK1 expression exacerbates HFD-induced obesity, adipocyte hypertrophy and inflammation

To test the effects of constitutive SGK1 activation on HFD-induced obesity, we fed 14-week-old wild type (WT) or Tg.sgk1 mice either with a standard chow diet (SCD) or a high-fat diet (HFD) for up to 6 weeks. At the end of this period mice fed SCD did not show any difference in total body weight, although Tg.sgk1 had a higher fat content, suggesting a predisposition to obesity (Table 3). HFD induced a faster weight gain in transgenics when compared to WT mice (Fig. 1A). The dramatic increase of BW gain in transgenic mice fed with HFD was not due to hyperphagia since food intake was even lower than WT mice (Fig. 1B). The observed BW differences were due to fat accumulation, as determined by DEXA (Fig. 1C and Table 3) or by individual dissection of fat pads (Fig. 1D). Histological analysis of epididymal adipose tissue revealed prominent adipocyte hypertrophy after 6 weeks of HFD in transgenic animals when compared to WT, with fewer adipocytes/area (Fig. 1E) and adipocyte area frequency distribution skewed towards larger values (Fig. 1F). Quantitative analysis of mRNA expression showed that white adipose tissue displays increased expression of SGK1, which is expected due to the increase gene dosage provided by the BAC insertion (Fig. 1G). Endogenously expressed Nedd4-2, a well-known SGK1 target (Debonneville, et al. 2001), showed increased phosphorylation in white adipose tissue from Tg.sgk1 mice when compared to WT, consistent with the expression of a constitutively active SGK1 (Fig. 1H). Adipocyte hypertrophy contributes to unfavorable metabolic changes (Sun, et al. 2011). To test whether fat pad expansion and adipocyte hypertrophy correlated with increased inflammation, we analyzed expression of inflammation markers in epididymal fat. No difference between WT and Tg.sgk1 mice was observed under SCD (Fig. 1I). HFD increased expression of all inflammation markers in both WT and Tg.sgk1 mice (Fig. 1I). However, Tg.sgk1 mice showed significantly higher expression of IL-6, TFNα and MCP-1, suggesting increased adipose tissue inflammation.

Constitutive activation of SGK1 promotes insulin-induced glucose and free fatty acids (FFA) uptake in primary adipocytes

To test whether adipocyte hypertrophy observed in Tg.sgk1 mice was due to increased nutrient uptake, we measured glucose and FFA uptake *in vitro* using differentiated adipocytes from adipose vascular stromal cells. Insulin-induced glucose and FFA uptake was higher in differentiated adipocytes derived from transgenic mice (Fig. 2A,B). At the molecular level, glucose transporter GLUT4 and lipid transporter CD36 expression levels were also significantly higher in cells derived from Tg.sgk1 mice (Fig. 2C,D), suggesting that SGK1 activation promotes adipocyte differentiation and lipid accumulation. This hypothesis was confirmed by the higher lipid accumulation (Fig. 2E,F) and adipogenesis marker expression (Fig. 2G) in cells derived from transgenic mice. Taken together, these data indicate that increased expression of SGK1 enhances adipogenesis and increases uptake of FFAs and glucose, possibly by up-regulating membrane transporters.

Dyslipidemia, glucose intolerance and insulin resistance in HFD-fed Tg.sgk1 mice

Adipocyte hypertrophy and low-grade inflammation are closely associated with the development of dyslipidemia and insulin resistance (Kim, et al. 2015; Shoelson, et al. 2006). To investigate whether the exacerbated obese phenotype observed in Tg.sgk1 mice correlated with larger metabolic disturbances, several metabolic parameters were measured in the plasma of SCD- or HFD-fed WT and Tg.sgk1 mice. Under fed conditions, HFD-fed transgenic mice showed significantly higher levels of insulin and triglycerides and decreased levels of HDL cholesterol (Table 3). Under fasting condition, Tg.sgk1 maintained their hyperinsulinemia as well as hyperglycemia (Table 3). In addition, SCD-fed transgenics also show increased fasting glucose (Table 3) and a positive correlation between glycemia and BW (Fig. 3A), suggesting an impairment of glucose homeostasis that is exacerbated under HFD. Accordingly, transgenic animals displayed a significantly impaired response to a glucose challenge after 5 weeks in HFD (Fig. 3B,C). ITT revealed that after 6 weeks in HFD Tg.sgk1 mice show decreased sensitivity to insulin (Fig. 3D,E). In agreement with these observations, HOMA index was increased in Tg.sgk1 compared to WT mice (Table 3). Transgenics also displayed decreased QUICKI values (Table 3). Analysis of insulinemia during GTT showed that glucose-stimulated insulin secretion was affected in

Accepted Manuscript published as JOE-19-0275.R1. Accepted for publication: 10-Oct-2019

Tg.sgk1 mice (Fig. 3F,G). This indicates that transgenic animals with excess SGK1 and fed a HFD are insulin resistant with advanced diabetic features.

Insulin resistance was further confirmed by studying the insulin signaling pathway in epididymal adipose tissue of HFD-fed animals. Despite significantly increased insulin receptor expression, Tg.sgk1 mice showed a significant reduction in phosphorylation of downstream effectors IRS1, protein kinase AKT and its substrate AS160 (Fig. 3H,I). This observation confirmed that defects responsible for insulin resistance occurred at the post-receptor level as previously described (Draznin 2006; Kolterman, et al. 1980).

Non-alcoholic fatty liver (NAFL) in HFD-fed Tg.sgk1 mice

In order to check whether the metabolic disorders induced by HFD in Tg.sgk1 mice accelerates the development of NAFL, we analyzed lipid accumulation by histological analysis of liver sections. We first confirmed increased SGK1 expression in the liver of transgenics. Total SGK1 mRNA abundance was increased by 60% in Tg.sgk1 compared to WT mice under SCD (Fig. 4A). Tg.sgk1 mice treated with HFD showed 2.8-fold increased expression of SGK1, suggesting that constitutively active SGK1 may potentiate its own expression under these conditions (Fig. 4A). Phosphorylation of a well-known downstream target of SGK1, glycogen synthase kinase 3 (GSK3) (Wyatt, et al. 2006), was also increased in Tg.sgk1 (Fig. 4B). Hematoxylin-eosin staining revealed that after 6 weeks of HFD Tg.sgk1 livers presented severe micro- and macro-vesicular steatosis with marked hepatocellular ballooning, while WT mice presented less affected livers with micro-vesicular steatosis only. Semiquantitative analysis of the extent of lipid inclusion supported widespread presence of NAFL in HFD-fed Tg.sgk1, but not in WT animals (Fig. 4C, D). Biochemical analysis of liver tissue composition confirmed the significantly higher triglycerides content in Tg.sgk1 mice livers (Fig. 4E).

HFD-fed Tg.sgk1 mice rapidly develop hypertension

To test whether SGK1 gain-of-function induces hypertension, we compared SBP measurements in WT and transgenic mice before and after HFD feeding. Animals kept in SCD did not show any differences on SBP between genotypes at 12 weeks of age (Fig. 5), or at later time points, even when challenged with

high NaCl intake (data not shown). Remarkably, HFD produced a significant increase on SBP in transgenic mice after 4 weeks of HFD. Tg.sgk1 SBP continued increasing over time to reach an average of 173 mmHg after 7 weeks on HFD and 184 mmHg after 18 weeks, approximately 40-50 mmHg higher than WT (Fig. 5). After 18 weeks of HFD WT animals also showed significantly elevated SBP when compared to animals on SCD (Fig. 5). Therefore, excess SGK1 sensitizes mice to rapidly developing hypertension when fed HFD.

Accepted Manuscript published as JOE-19-0275.R1. Accepted for publication: 10-Oct-2019

DISCUSSION

SGK1 as a risk factor for obesity and MetS

Available information strongly supports the idea that SGK1 constitutes a convergence point linking obesity, metabolic alterations and hypertension, all clustered in the so-called MetS. From a mechanistic standpoint, these effects appeared to be multifactorial (see below). Therefore, our mouse model with systemic SGK1 expression under its own promoter but harboring a gain-of-function mutation appeared ideally suited to evaluate the role of this kinase in a complex and multi-organ condition such as the MetS. We found that excess SGK1 activity promotes adiposity together with hyperglycemia under a standard chow diet. The full deleterious effects of SGK1 were triggered by increased fat intake, leading to a very rapid and prominent development of other MetS components, most notably hypertension. This conclusion validates our hypothesis that a systemic increase in SGK1 activity constitutes a risk factor for metabolic disorders progression.

The adipose tissue was considered for a long time to be a passive fat storage compartment, but nowadays it is regarded as a versatile and central organ in the development of metabolic disorders. SGK1 is overexpressed in adipose tissue in obese mice and humans (Li, et al. 2013) and it participates in HFD-induced adipogenesis (Ding, et al. 2017). Our results using a gain-of-function SGK1 mutation support the involvement of SGK1 in adipocyte differentiation *in vitro*, as previously described in *Sgk1* knockout mouse model (Di Pietro et al. 2010). We found that activated SGK1 promotes lipid accumulation within the cytoplasm, probably due to increased glucose and FFA uptake. However, the role of SGK1 in energy metabolism is likely not restricted to adipocytes. SGK1 is also expressed in the liver, where it has been shown to regulate insulin sensitivity (Liu, et al. 2014). Our data also suggests hepatic effects of SGK1, based on the hypertriglyceridemia detected under HFD and also the rapid development of NAFL. However, additional investigations are needed to decipher whether SGK1 has a direct effect on hepatocytes or an indirect effect related to the observed dyslipidemia leading to ectopic fat deposition. In skeletal muscle, SGK1 appears to be involved in increasing glucose transporter expression, glucose

uptake and glycogen accumulation (Singh, et al. 2013). Finally, a recent report showed that specific deletion of *Sgk1* in *POMC* neurons increases adiposity induced by glucocorticoids (Deng, et al. 2018).

The metabolic roles of SGK1 are added to its role in renal Na^+ handling and blood pressure control. *Sgk1* knockout animals do not shown altered SBP under normal conditions, but display impaired aldosterone-mediated increase in Na^+ reabsorption, leading to decreased blood pressure under low salt intake (Faresse, et al. 2012; Wulff et al. 2002). SGK1 mediates the synergistic effect of insulin on aldosterone-induced Na^+ reabsorption through the epithelial Na^+ channel (Alvarez de la Rosa and Canessa 2003; Wang, et al. 2001). Recently, Norlander et al, showed that specific deletion of SGK1 in T cells blunts the increase in blood pressure in both the angiotensin II and DOCA/salt models of hypertension (Norlander et al. 2017), pointing to a multiplicity of mechanisms by which SGK1 may regulate blood pressure. Crucially, SGK1 knockout mice are protected against salt-dependent hypertension in the context of a high-fat (Huang et al. 2006b) or high-fructose diets (Huang, et al. 2006a). In addition, SGK1 polymorphisms associate to increased blood pressure in humans (Busjahn et al. 2002), making carriers more susceptible to blood pressure increase associated to hyperinsulinemia (von Wowern et al. 2005). Our results represent the first analysis of increased SGK1 effects on blood pressure. In the absence of a challenge, SBP in transgenic animals is indistinguishable from WT. However, HFD produced a very rapid and large increase in blood pressure, in agreement with the notion that excess SGK1 activity may constitute a risk factor to develop hyperinsulinemia-related hypertension. Remarkably, in the absence of obesity and metabolic disturbances, a high-salt intake challenge did not raise SBP, suggesting that the coordinated activity of SGK1 in different tissues, and not just in the kidney, is responsible for this effect. The effects of increased SGK1 activity on blood pressure after a combined challenge of high-salt and high-fat intake remains to be determined.

The relevant upstream stimuli upregulating SGK1 expression in adipose tissue of mouse models of obesity as well as obese and diabetic patients remain elusive (Li et al. 2013). Transcription of this kinase is regulated by several factors, including corticosteroids acting through the glucocorticoid and mineralocorticoid receptors (GR and MR, respectively) (Chen et al. 1999; Naray-Fejes-Toth et al. 1999;

Accepted Manuscript published as JOE-19-0275.R1. Accepted for publication: 10-Oct-2019

Webster et al. 1993). Systemic glucocorticoid excess such as during Cushing syndrome reproduce the main characteristics of MetS (Newell-Price, et al. 2006). Several lines of evidence support a key role for both GR and MR in the pathogenesis of MetS by acting on several targets including the adipocyte, although there is conflicting evidence regarding the relative roles of each on adipocyte differentiation and function (Desarzens and Faresse 2016; Gomez-Sanchez 2015; Lee, et al. 2014; Marzolla, et al. 2012; Urbanet, et al. 2015). Remarkably, the use of a combined GR/MR antagonist significantly reduced the development of obesity in mice under HFD (Mammi, et al. 2016). Our results suggest that at least some of the deleterious effects of GR/MR activation may be mediated through SGK1.

SGK1 inhibition as a possible strategy to treat obesity-related hypertension

Our study, together with previously available evidence, suggests that SGK1 is a potential target to treat obesity-induced hypertension. HFD-fed *Sgk1* knockout mice are resistant to salt-sensitive hypertension, but not to hypertension induced by HFD alone (Huang et al. 2006b). Similarly, *Sgk1* knockout mice are resistant to moderate increases in blood pressure induced by combined high-fructose and high-salt intake (Huang et al. 2006a), suggesting that the hypertensive effect of hyperinsulinemia may be associated to SGK1. In this context, preliminary studies using the SGK1 inhibitor EMD638683 lowered blood pressure in mice fed a high-fructose, high-salt diet (Ackermann et al. 2011). Furthermore, SGK1 inhibition showed beneficial effects in the development of obesity and hyperglycemia in *db/db* mice (Li et al. 2016). However, *Sgk1* knockout mice also show glucose intolerance and insulin resistance (Huang et al. 2006b), which could present a problem in long-term treatments inhibiting the kinase. In addition, the development of SGK1 inhibitors would have to overcome cross-reactivity with related kinases, including isoforms SGK2, SGK3 and AKT (Ackermann et al. 2011).

A new mouse model for MetS, related comorbidities and end organ damage

One important observation made in this study is that HFD-fed Tg.sgk1 mice develop MetS features closer to the ones observed in humans, more rapidly and prominently than most available models. The availability of suitable rodent models to study the pathophysiological and molecular mechanisms of MetS progression is limited and most of them do not exhibit the entire clinical features observed in humans.

The existing mouse models of MetS present several shortcomings, including the inconsistency of hypertension development in obese mice (Kennedy, et al. 2010). Most models show coincident obesity and insulin resistance. However, the simultaneous presence of these two characteristics with dyslipidemia and hypertension is more difficult to achieve. In WT mice, 4 months of HFD raised the systolic blood pressure by 30-40 mmHg, confirming previous studies (Gupte, et al. 2008; Marshall, et al. 2013), although in other reports even this long treatment is not enough to raise blood pressure (Police, et al. 2009). In Tg.sgk1 mice, a similar increase was reached after only 4 weeks of HFD and dramatically increased at longer time points. In addition to hypertension, all features of MetS appeared faster and more severe in our model. NAFL, a comorbidity commonly co-existing with MetS and hypertension (Cornier, et al. 2008), is also accelerated in our model. Our results and other studies showed that 6 weeks of HFD has no effect on hepatic triglyceride levels in WT mice (Nam, et al. 2015; Yamaguchi, et al. 2007). In contrast, the same period of high-fat feeding induces hepatic triglycerides accumulation in Tg.sgk1 comparable to levels found in C57BL/6 mice after 12 weeks in HFD (Nam et al. 2015).

Limitations of this study and perspectives

For practical reasons, our study included only male mice. Based on the known sexual dimorphism in susceptibility to obesity in mice (Hong, et al. 2009), additional experiments are needed to test the effects of excess SGK1 activity on female mice. Also, it should be noted that a common weakness in studies using HFD vs. standard chow is that diets are not isocaloric and matched for ingredients. Therefore, other ingredients varying between diets may also contribute to the phenotype described here. Most importantly, the effects of SGK1 described here are likely due to synergistic mechanisms affecting among others energy storage, insulin signaling and renal Na^+ handling. Dissection of the relative importance of these mechanisms will need the development of tissue-specific conditional SGK1 gain-of-function models together with already available *Sgk1* knockout lines.

From a translational perspective, our data further supports the idea of SGK1 as a possible therapeutic target in MetS, particularly in situations where obesity co-exists with hypertension. Due to the fast and complete development of MetS with hypertension after a short HFD treatment, we propose that

Accepted Manuscript published as JOE-19-0275.R1. Accepted for publication: 10-Oct-2019

344 the SGK1 systemic gain-of-function model constitutes a useful experimental in vivo model for pre-
345 clinical drug testing.

Declaration of interests: The authors report no conflicts of interest in this work.

Funding: This study was funded by Ministerio de Economía y Competitividad (BFU2016-78374-R) and Agencia Canaria de Investigación, Innovación y Sociedad de la Información (ProID2017010135) to D.A.R. C.S.-R. was partially supported by Campus de Excelencia Regional (Universidad de La Laguna, Spain). S.V.-G. was supported by Programa Agustín de Betancourt (Cabildo de Tenerife, Spain).

Acknowledgments. We thank Dr. Dawn E.W. Livingstone (University of Edinburgh) for advice on glucose homeostasis assessment, Dr. Lucio Díaz-Flores and Dr. Ricardo Gutiérrez (University of La Laguna) for advice on tissue histology, Dr. Johannes Loffing (University of Zurich) for the kind gift of reagents and the Histology Facility at Centro Nacional de Biotecnología (Consejo Superior de Investigaciones Científicas, Spain) for preparation of tissue sections.

Accepted Manuscript published as JOE-19-0275.R1. Accepted for publication: 10-Oct-2019

REFERENCES

Ackermann TF, Boini KM, Beier N, Scholz W, Fuchss T & Lang F 2011 EMD638683, a novel SGK inhibitor with antihypertensive potency. *Cell Physiol Biochem* **28** 137-146.

Alvarez de la Rosa D & Canessa CM 2003 Role of SGK in hormonal regulation of epithelial sodium channel in A6 cells. *Am J Physiol Cell Physiol* **284** C404-414.

Andres-Mateos E, Brinkmeier H, Burks TN, Mejias R, Files DC, Steinberger M, Soleimani A, Marx R, Simmers JL, Lin B, et al. 2013 Activation of serum/glucocorticoid-induced kinase 1 (SGK1) is important to maintain skeletal muscle homeostasis and prevent atrophy. *EMBO Mol Med* **5** 80-91.

Artunc F & Lang F 2014 Mineralocorticoid and SGK1-sensitive inflammation and tissue fibrosis. *Nephron Physiol* **128** 35-39.

Bowe JE, Franklin ZJ, Hauge-Evans AC, King AJ, Persaud SJ & Jones PM 2014 Metabolic phenotyping guidelines: assessing glucose homeostasis in rodent models. *J Endocrinol* **222** G13-25.

Brunet A, Park J, Tran H, Hu LS, Hemmings BA & Greenberg ME 2001 Protein kinase SGK mediates survival signals by phosphorylating the forkhead transcription factor FKHRL1 (FOXO3a). *Mol Cell Biol* **21** 952-965.

Busjahn A, Aydin A, Uhlmann R, Krasko C, Bahring S, Szelestei T, Feng Y, Dahm S, Sharma AM, Luft FC, et al. 2002 Serum- and glucocorticoid-regulated kinase (SGK1) gene and blood pressure. *Hypertension* **40** 256-260.

Chen SY, Bhargava A, Mastroberardino L, Meijer OC, Wang J, Buse P, Firestone GL, Verrey F & Pearce D 1999 Epithelial sodium channel regulated by aldosterone-induced protein sgk. *Proc Natl Acad Sci U S A* **96** 2514-2519.

Cornier MA, Dabelea D, Hernandez TL, Lindstrom RC, Steig AJ, Stob NR, Van Pelt RE, Wang H & Eckel RH 2008 The metabolic syndrome. *Endocr Rev* **29** 777-822.

Debonneville C, Flores SY, Kamynina E, Plant PJ, Tauxe C, Thomas MA, Munster C, Chraibi A, Pratt JH, Horisberger JD, et al. 2001 Phosphorylation of Nedd4-2 by Sgk1 regulates epithelial Na(+) channel cell surface expression. *EMBO J* **20** 7052-7059.

Deng Y, Xiao Y, Yuan F, Liu Y, Jiang X, Deng J, Fejes-Toth G, Naray-Fejes-Toth A, Chen S, Chen Y, et al. 2018 SGK1/FOXO3 Signaling in Hypothalamic POMC Neurons Mediates Glucocorticoid-Increased Adiposity. *Diabetes*.

Desarzens S & Faresse N 2016 Adipocyte glucocorticoid receptor has a minor contribution in adipose tissue growth. *J Endocrinol* **230** 1-11.

Di Pietro N, Panel V, Hayes S, Bagattin A, Meruvu S, Pandolfi A, Hugendubler L, Fejes-Toth G, Naray-Fejes-Toth A & Mueller E 2010 Serum- and glucocorticoid-inducible kinase 1 (SGK1) regulates adipocyte differentiation via forkhead box O1. *Mol Endocrinol* **24** 370-380.

Dieter M, Palmada M, Rajamanickam J, Aydin A, Busjahn A, Boehmer C, Luft FC & Lang F 2004 Regulation of glucose transporter SGLT1 by ubiquitin ligase Nedd4-2 and kinases SGK1, SGK3, and PKB. *Obes Res* **12** 862-870.

Ding L, Zhang L, Biswas S, Schugar RC, Brown JM, Byzova T & Podrez E 2017 Akt3 inhibits adipogenesis and protects from diet-induced obesity via WNK1/SGK1 signaling. *JCI Insight* **2**.

Draznin B 2006 Molecular mechanisms of insulin resistance: serine phosphorylation of insulin receptor substrate-1 and increased expression of p85alpha: the two sides of a coin. *Diabetes* **55** 2392-2397.

Faresse N, Lagnaz D, Debonneville A, Ismailji A, Maillard M, Fejes-Toth G, Naray-Fejes-Toth A & Staub O 2012 Inducible kidney-specific Sgk1 knockout mice show a salt-losing phenotype. *Am J Physiol Renal Physiol* **302** F977-985.

Garcia-Martinez JM & Alessi DR 2008 mTOR complex 2 (mTORC2) controls hydrophobic motif phosphorylation and activation of serum- and glucocorticoid-induced protein kinase 1 (SGK1). *Biochem J* **416** 375-385.

Gomez-Sanchez CE 2015 What Is the Role of the Adipocyte Mineralocorticoid Receptor in the Metabolic Syndrome? *Hypertension* **66** 17-19.

Accepted Manuscript published as JOE-19-0275.R1. Accepted for publication: 10-Oct-2019

405 Gupte M, Boustany-Kari CM, Bharadwaj K, Police S, Thatcher S, Gong MC, English VL & Cassis LA
406 2008 ACE2 is expressed in mouse adipocytes and regulated by a high-fat diet. *Am J Physiol Regul Integr*
407 *Comp Physiol* **295** R781-788.
408 Hong J, Stubbins RE, Smith RR, Harvey AE & Nunez NP 2009 Differential susceptibility to obesity
409 between male, female and ovariectomized female mice. *Nutr J* **8** 11.
410 Huang DY, Boini KM, Friedrich B, Metzger M, Just L, Osswald H, Wulff P, Kuhl D, Vallon V & Lang F
411 2006a Blunted hypertensive effect of combined fructose and high-salt diet in gene-targeted mice lacking
412 functional serum- and glucocorticoid-inducible kinase SGK1. *Am J Physiol Regul Integr Comp Physiol*
413 **290** R935-944.
414 Huang DY, Boini KM, Osswald H, Friedrich B, Artunc F, Ullrich S, Rajamanickam J, Palmada M, Wulff
415 P, Kuhl D, et al. 2006b Resistance of mice lacking the serum- and glucocorticoid-inducible kinase SGK1
416 against salt-sensitive hypertension induced by a high-fat diet. *Am J Physiol Renal Physiol* **291** F1264-
417 1273.
418 Kennedy AJ, Ellacott KL, King VL & Hasty AH 2010 Mouse models of the metabolic syndrome. *Dis*
419 *Model Mech* **3** 156-166.
420 Kim JI, Huh JY, Sohn JH, Choe SS, Lee YS, Lim CY, Jo A, Park SB, Han W & Kim JB 2015 Lipid-
421 overloaded enlarged adipocytes provoke insulin resistance independent of inflammation. *Mol Cell Biol* **35**
422 1686-1699.
423 Kleiner DE, Brunt EM, Van Natta M, Behling C, Contos MJ, Cummings OW, Ferrell LD, Liu YC,
424 Torbenson MS, Unalp-Arida A, et al. 2005 Design and validation of a histological scoring system for
425 nonalcoholic fatty liver disease. *Hepatology* **41** 1313-1321.
426 Kobayashi T & Cohen P 1999 Activation of serum- and glucocorticoid-regulated protein kinase by
427 agonists that activate phosphatidylinositide 3-kinase is mediated by 3-phosphoinositide-dependent protein
428 kinase-1 (PDK1) and PDK2. *Biochem J* **339 (Pt 2)** 319-328.
429 Kolterman OG, Insel J, Saekow M & Olefsky JM 1980 Mechanisms of insulin resistance in human
430 obesity: evidence for receptor and postreceptor defects. *J Clin Invest* **65** 1272-1284.

Lang F, Bohmer C, Palmada M, Seebohm G, Strutz-Seebohm N & Vallon V 2006 (Patho)physiological significance of the serum- and glucocorticoid-inducible kinase isoforms. *Physiol Rev* **86** 1151-1178.

Lee M, Fried S, Armani Rt, Lee M, Fried S & Armani Rt 2014 Can cortisol stimulate adipogenesis without the glucocorticoid receptor? *International Journal of Obesity* **38** 1578-1579.

Li P, Hao Y, Pan FH, Zhang M, Ma JQ & Zhu DL 2016 SGK1 inhibitor reverses hyperglycemia partly through decreasing glucose absorption. *J Mol Endocrinol* **56** 301-309.

Li P, Pan F, Hao Y, Feng W, Song H & Zhu D 2013 SGK1 is regulated by metabolic-related factors in 3T3-L1 adipocytes and overexpressed in the adipose tissue of subjects with obesity and diabetes. *Diabetes Res Clin Pract* **102** 35-42.

Liu H, Yu J, Xia T, Xiao Y, Zhang Q, Liu B, Guo Y, Deng J, Deng Y, Chen S, et al. 2014 Hepatic serum- and glucocorticoid-regulated protein kinase 1 (SGK1) regulates insulin sensitivity in mice via extracellular-signal-regulated kinase 1/2 (ERK1/2). *Biochem J* **464** 281-289.

Mammi C, Marzolla V, Armani A, Feraco A, Antelmi A, Maslak E, Chlopicki S, Cinti F, Hunt H, Fabbri A, et al. 2016 A novel combined glucocorticoid-mineralocorticoid receptor selective modulator markedly prevents weight gain and fat mass expansion in mice fed a high-fat diet. *Int J Obes (Lond)* **40** 964-972.

Marshall NJ, Liang L, Bodkin J, Dessapt-Baradez C, Nandi M, Collot-Teixeira S, Smillie SJ, Lalgi K, Fernandes ES, Gnudi L, et al. 2013 A role for TRPV1 in influencing the onset of cardiovascular disease in obesity. *Hypertension* **61** 246-252.

Marzolla V, Armani A, Zennaro MC, Cinti F, Mammi C, Fabbri A, Rosano GM & Caprio M 2012 The role of the mineralocorticoid receptor in adipocyte biology and fat metabolism. *Mol Cell Endocrinol* **350** 281-288.

Miranda P, Cadaveira-Mosquera A, Gonzalez-Montelongo R, Villarroel A, Gonzalez-Hernandez T, Lamas JA, Alvarez de la Rosa D & Giraldez T 2013 The neuronal serum- and glucocorticoid-regulated kinase 1.1 reduces neuronal excitability and protects against seizures through upregulation of the M-current. *J Neurosci* **33** 2684-2696.

Accepted Manuscript published as JOE-19-0275.R1. Accepted for publication: 10-Oct-2019

456 Muniyappa R, Lee S, Chen H & Quon MJ 2008 Current approaches for assessing insulin sensitivity and
457 resistance in vivo: advantages, limitations, and appropriate usage. *Am J Physiol Endocrinol Metab* **294**
458 E15-26.
459 Nam M, Choi MS, Jung S, Jung Y, Choi JY, Ryu DH & Hwang GS 2015 Lipidomic Profiling of Liver
460 Tissue from Obesity-Prone and Obesity-Resistant Mice Fed a High Fat Diet. *Sci Rep* **5** 16984.
461 Naray-Fejes-Toth A, Canessa C, Cleaveland ES, Aldrich G & Fejes-Toth G 1999 sgk is an aldosterone-
462 induced kinase in the renal collecting duct. Effects on epithelial na+ channels. *J Biol Chem* **274** 16973-
463 16978.
464 Newell-Price J, Bertagna X, Grossman AB & Nieman LK 2006 Cushing's syndrome. *Lancet* **367** 1605-
465 1617.
466 Norlander AE, Saleh MA, Pandey AK, Itani HA, Wu J, Xiao L, Kang J, Dale BL, Goleva SB,
467 Laroumanie F, et al. 2017 A salt-sensing kinase in T lymphocytes, SGK1, drives hypertension and
468 hypertensive end-organ damage. *JCI Insight* **2**.
469 Pacini G, Omar B & Ahren B 2013 Methods and models for metabolic assessment in mice. *J Diabetes*
470 *Res* **2013** 986906.
471 Pearce D 2003 SGK1 regulation of epithelial sodium transport. *Cell Physiol Biochem* **13** 13-20.
472 Police SB, Thatcher SE, Charnigo R, Daugherty A & Cassis LA 2009 Obesity promotes inflammation in
473 periaortic adipose tissue and angiotensin II-induced abdominal aortic aneurysm formation. *Arterioscler*
474 *Thromb Vasc Biol* **29** 1458-1464.
475 Schwab M, Lupescu A, Mota M, Mota E, Frey A, Simon P, Mertens PR, Floege J, Luft F, Asante-Poku S,
476 et al. 2008 Association of SGK1 gene polymorphisms with type 2 diabetes. *Cell Physiol Biochem* **21** 151-
477 160.
478 Shoelson SE, Lee J & Goldfine AB 2006 Inflammation and insulin resistance. *J Clin Invest* **116** 1793-
479 1801.

480 Singh PK, Singh S & Ganesh S 2013 Activation of serum/glucocorticoid-induced kinase 1 (SGK1)
481 underlies increased glycogen levels, mTOR activation, and autophagy defects in Lafora disease. *Mol Biol*
482 *Cell* **24** 3776-3786.
483 Sun K, Kusminski CM & Scherer PE 2011 Adipose tissue remodeling and obesity. *J Clin Invest* **121**
484 2094-2101.
485 Urbanet R, Nguyen Dinh Cat A, Feraco A, Venteclef N, El Mogrhabi S, Sierra-Ramos C, Alvarez de la
486 Rosa D, Adler GK, Quilliot D, Rossignol P, et al. 2015 Adipocyte Mineralocorticoid Receptor Activation
487 Leads to Metabolic Syndrome and Induction of Prostaglandin D2 Synthase. *Hypertension* **66** 149-157.
488 Verrey F, Loffing J, Zecevic M, Heitzmann D & Staub O 2003 SGK1: aldosterone-induced relay of Na+
489 transport regulation in distal kidney nephron cells. *Cell Physiol Biochem* **13** 21-28.
490 von Wowern F, Berglund G, Carlson J, Mansson H, Hedblad B & Melander O 2005 Genetic variance of
491 SGK-1 is associated with blood pressure, blood pressure change over time and strength of the insulin-
492 diastolic blood pressure relationship. *Kidney Int* **68** 2164-2172.
493 Wang J, Barbry P, Maiyar AC, Rozansky DJ, Bhargava A, Leong M, Firestone GL & Pearce D 2001
494 SGK integrates insulin and mineralocorticoid regulation of epithelial sodium transport. *Am J Physiol*
495 *Renal Physiol* **280** F303-313.
496 Webster MK, Goya L, Ge Y, Maiyar AC & Firestone GL 1993 Characterization of sgk, a novel member
497 of the serine/threonine protein kinase gene family which is transcriptionally induced by glucocorticoids
498 and serum. *Mol Cell Biol* **13** 2031-2040.
499 Wulff P, Vallon V, Huang DY, Volkl H, Yu F, Richter K, Jansen M, Schlunz M, Klingel K, Loffing J, et
500 al. 2002 Impaired renal Na(+) retention in the sgk1-knockout mouse. *J Clin Invest* **110** 1263-1268.
501 Wyatt AW, Hussain A, Amann K, Klingel K, Kandolf R, Artunc F, Grahammer F, Huang DY, Vallon V,
502 Kuhl D, et al. 2006 DOCA-induced phosphorylation of glycogen synthase kinase 3beta. *Cell Physiol*
503 *Biochem* **17** 137-144.

Accepted Manuscript published as JOE-19-0275.R1. Accepted for publication: 10-Oct-2019

504 Yamaguchi K, Yang L, McCall S, Huang J, Yu XX, Pandey SK, Bhanot S, Monia BP, Li YX & Diehl
505 AM 2007 Inhibiting triglyceride synthesis improves hepatic steatosis but exacerbates liver damage and
506 fibrosis in obese mice with nonalcoholic steatohepatitis. *Hepatology* **45** 1366-1374.

FIGURES LEGENDS

Figure 1. Constitutively active SGK1 exacerbates diet-induced obesity, adipocyte hypertrophy and adipose tissue inflammation. A, BW variation in aged-matched WT or Tg.sgk1 mice fed with a high-fat diet (HFD). Data points represent average weekly cumulative weight gain ± SE (N=39 for WT; N=43 for Tg.sgk1). Two-way ANOVA followed by Tukey's multiple comparison test (*p<0.05, ***p<0.001). **B**, Average ± SEM food intake/day in animals fed with SCD or HFD (N=5 for SCD; N=15 for WT HFD group; N=18 for Tg.sgk1 HFD; **p<0.01, Student´s t test). **C**, Representative images of body composition analysis by DEXA in anesthetized mice. **D**, Average epididymal and mesenteric adipose tissue weight ± SEM (N=6) normalized to total body weight of WT and Tg.sgk1 mice kept on SCD or after 6 weeks on HFD (*p<0.05, ***p<0.001, ****p<0.0001, one-way ANOVA followed by Tukey's multiple comparison test). The weight of inguinal fat in mice kept in SCD was not determined (n.d.). **E**, Representative micrographs of hematoxylin-eosin stained epididymal white adipose tissue obtained from WT or Tg.sgk1 mice kept under SCD or fed a HFD for 6 weeks. Bar, 40 μm. **F**, Frequency histogram with Gaussian distribution fit showing percentage of adipocytes from HFD-fed animals in each area category (N=6). Dashed lines, median values for WT and Tg.sgk1 adipocyte area. ***p<0.001, Mann-Whitney test. **G**, SGK1 mRNA expression in epididymal fat of WT and Tg.sgk1 mice under SCD or HFD. Values represent average ± SEM (N=6). *p<0.05, one-way ANOVA followed by Sidak's multiple comparison test. **H**, Representative immunoblot detecting total and phospho-S488 Nedd4-2 in protein extracts obtained from epididymal fat of WT or Tg.sgk1 mice. **I**, Relative mRNA expression of inflammation markers in epididymal fat of WT and Tg.sgk1 mice under SCD or HFD. Values represent average ± SEM (N=6). nd, non-detectable. IL-1, interleukin 1; IL-6, interleukin 6; TNFα, tumor necrosis factor α; CD68, cluster of differentiation 68; MCP1, monocyte chemoattractant protein-1. *p<0.05, **p<0.01, one-way ANOVA followed by Sidak's multiple comparison test.

Figure 2. Increased SGK1 increases glucose and free fatty acids (FAA) uptake and accelerates *in vitro* adipocyte differentiation. Basal and insulin-induced glucose (**A**) or FAA (**B**) uptake in undifferentiated and differentiated adipocytes obtained from WT or Tg.sgk1 mice. Bars represent average

Accepted Manuscript published as JOE-19-0275.R1. Accepted for publication: 10-Oct-2019

534 ± SEM (N=4) incorporated radioactivity normalized to protein concentration. Student's t test, *p<0.05.
535 Glucose transporter GLUT4 (**C**) and lipid transporter CD36 (**D**) mRNA expression at Day 0 and Day 7
536 during differentiation. Values are average ± SEM (N=4). Student's t test; **, p<0.01. **E**, Oil red-O
537 accumulation in undifferentiated or differentiated cells. **F**, Symbols represent individual oil red-O
538 absorbance values at 520 nm from four independent experiments; *, p<0.05; ***, p<0.001 (two-way
539 ANOVA followed by Sidak's multiple comparison test). **G**, Lipogenic marker expression during
540 differentiation. Values are average ± SEM normalized to RPL13A. PPARγ, peroxisome proliferator
541 activated receptor γ; CEBPα, CCAAT-enhancer binding protein α; LPL, lipoprotein lipase. Two-way
542 ANOVA followed by Sidak's multiple comparison test: *, p<0.05; **, p<0.01; ***, p<0.001.
543 **Figure 3. Tg.*sgk1* mice show impaired glucose tolerance and insulin resistance. A**, Positive
544 correlation between body weight and fasting glycemia in Tg.sgk1, but not in WT mice fed SCD.
545 Spearman correlation: WT, p=0.084; Tg.sgk1, p=0.029. Linear correlation slope in Tg.sgk1=3.9±1.6
546 (p=0.03); linear correlation slope in WT mice was not significantly different from zero (p=0.128). **B**,
547 Glucose tolerance test (GTT) in WT and Tg.sgk1 kept in SCD or fed HFD for 5 weeks. Values are
548 average glycemia ± SEM at the indicated time point after glucose load (N=14; WT SCD; N=13, Tg.sgk1
549 SCD; N=23, WT HFD; N=26, Tg.sgk1 HFD). Two-way ANOVA followed by Tukey´s multiple
550 comparison test (Tg.sgk1 HFD vs. Tg.sgk1 SCD, *p<0.05; Tg.sgk1 HFD vs. WT HFD, #p<0.05; WT
551 HFD vs. WT SCD, &p<0.05; Tg.sgk1 SCD vs. WT SCD, +p<0.05; for simplicity the other three
552 comparisons are not shown). **C**, Individual points represent area under the curve (AUC) values obtained
553 from each mice in the GTT curves shown in panel B. Average ± SEM AUC are also indicated. One-way
554 ANOVA followed by Tukey's multiple comparison test: **p<0.01, ***p<0.001). **D**, Insulin Tolerance
555 Test (ITT). Values represent average glycemia ± SEM (N=16) at the indicated time point after insulin
556 injection. Two-way ANOVA followed by Tukey´s multiple comparison test (Tg.sgk1 HFD vs. Tg.sgk1
557 SCD, *p<0.05; Tg.sgk1 HFD vs. WT HFD, #p<0.05; WT HFD vs. WT SCD, &p<0.05; for simplicity the
558 other three comparisons are not shown; there were no significant differences between Tg.sgk1 and WT in
559 SCD). **E**, Individual points represent area under the curve (AUC) values obtained from each mice in the

ITT curves shown in panel D. Average ± SEM AUC are also indicated. One-way ANOVA followed by Tukey's multiple comparison test; (*p<0.05, **p<0.01, ***p<0.001). **F**, Average insulinemia ± SEM at the indicated time points during GTT in mice fed with SCD or with HFD for 5 weeks (N=7, WT; N=11, Tg.sgk1). Two-way ANOVA followed by Tukey's multiple comparison test: Tg.sgk1 HFD vs. Tg.sgk1 SCD, **p<0.01, ***p<0.001; Tg.sgk1 HFD vs. WT SCD, ++p<0.01, +++p<0.001; Tg.sgk1 HFD vs. WT HFD, ##p<0.01, ###p<0.001. **G**, Individual points represent area under the curve (AUC) values obtained from each mice in the insulinemia curves shown in panel F. Average ± SEM AUC are also indicated. One-way ANOVA followed by Tukey's multiple comparison test; (*p<0.05, **p<0.01, ***p<0.001). **H**, Insulin signaling pathway analyzed by western blot of epididymal adipose tissue from WT and Tg.sgk1 mice after 6 weeks on HFD (N=5). Each lane corresponds to a sample from one animal. InsR, insulin receptor; IRS1, insulin receptor substrate 1; AS160, AKT substrate of 160 kDa. **I**, Quantitative analysis of western blots shown in panel H. Values represents average ± SEM (Student's t test, *p<0.05).

Figure 4. HFD produces liver steatosis in Tg.sgk1 mice. A, Relative SGK1 mRNA expression in liver of WT and Tg.sgk1 mice under SCD or HFD. Values represent average ± SEM (N=5-7). *p<0.05, one-way ANOVA followed by Sidak's multiple comparison test. **B**, Representative immunoblot detecting phosphorylated GSK3β at residue S9 and total GSK-3β in liver protein extracts from three different WT and Tg.sgk1 mice. **C**, Representative images of hematoxylin-eosin-stained liver sections from WT or Tg.sgk1 mice fed a HFD for 6 weeks. **D**, Semiquantitative analysis of lipid deposition in liver sections. Each bar represents the percentage of animals included in each score category (-, no lipid drops; +, ++, +++, increasing amounts of lipid drops). N=6. **E**, Hepatic triglyceride content. Bars represent average ± SEM normalized to tissue weight (N=7, WT; N=9, Tg.sgk1). *p<0.05, Student's t test.

Figure 5. Excess SGK1 activity induces hypertension in HFD-fed mice. Individual points represent systolic blood pressure (SBP) obtained using the tail-cuff method on 12-week-old WT and Tg.sgk1 mice kept on SCD or after the indicated time on HFD (N=9, SCD; N=10, HFD, 4 weeks; N=7, WT HFD, 7 weeks; N=11, Tg.sgk1 HFD, 7 weeks; N=4, WT HFD, 18 weeks; N=6, Tg.sgk1 HFD, 18 weeks). Average values ± SEM are also represented. Two-way ANOVA followed by Bonferroni´s multiple

Accepted Manuscript published as JOE-19-0275.R1. Accepted for publication: 10-Oct-2019

586 comparison test (WT vs. Tg.sgk1: n.s., no significant difference; *p<0.05; **p<0.01; ***p<0.001.

587 +p<0.05, WT SCD vs. WT 18 weeks HFD. #p<0.05, ###p<0.001, Tg.sgk1 SCD vs. HFD).

Accepted Manuscript published as JOE-19-0275.R1. Accepted for publication: 10-Oct-2019

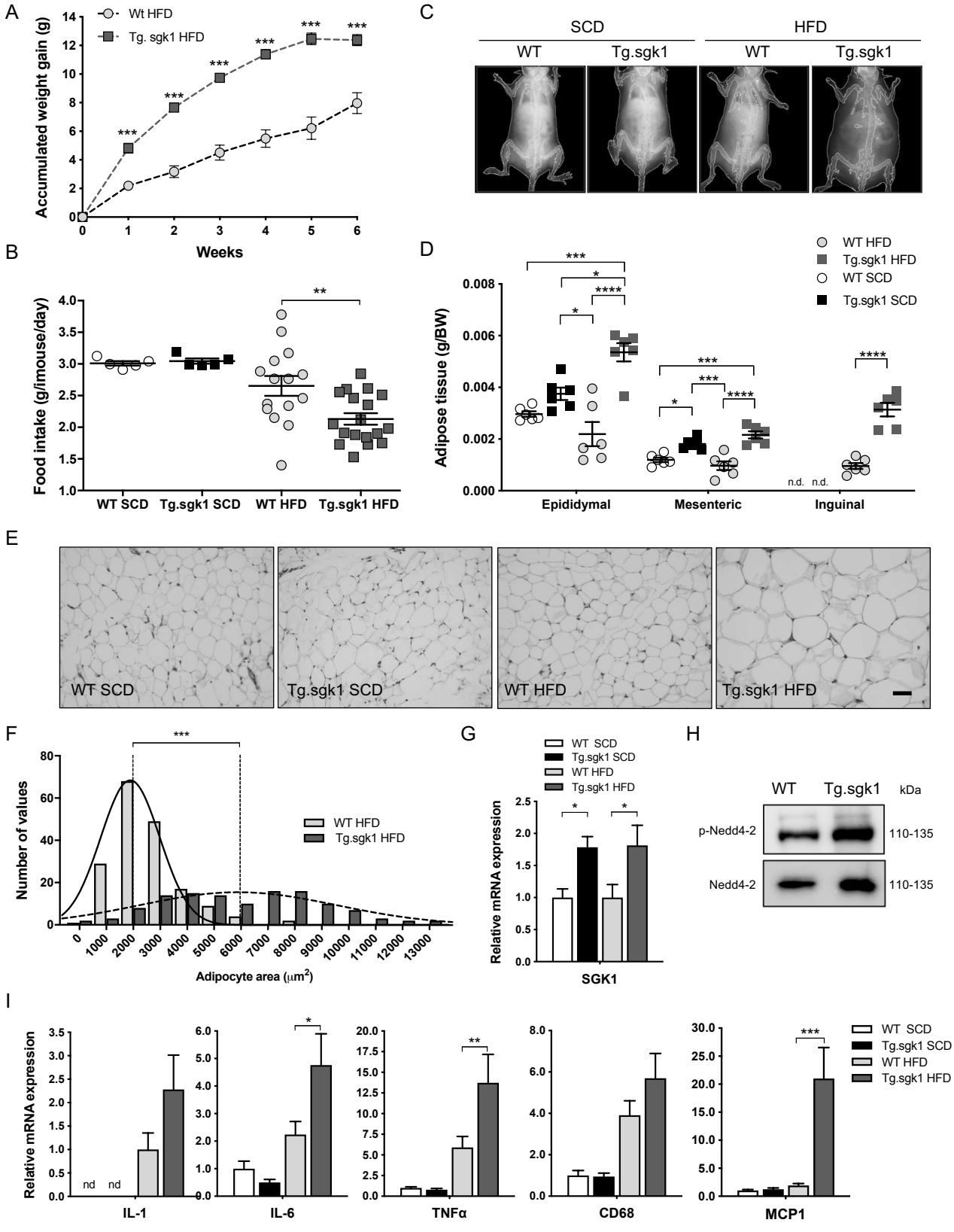

 Accepted Manuscript published as JOE-19-0275.R1. Accepted for publication: 10-Oct-2019

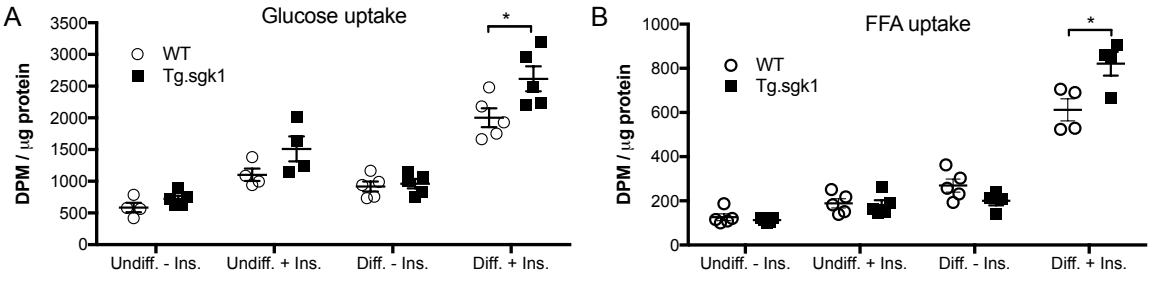

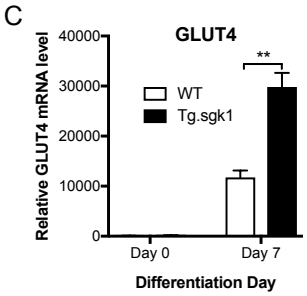

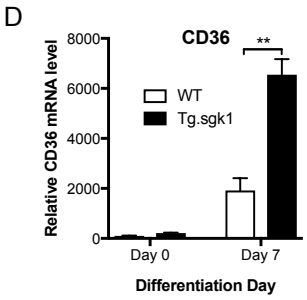

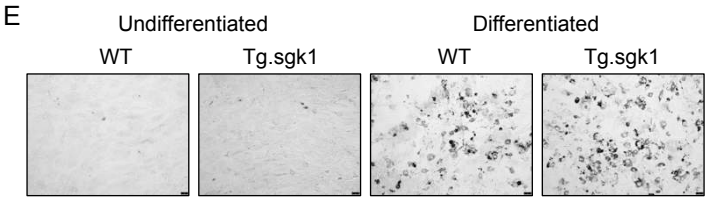

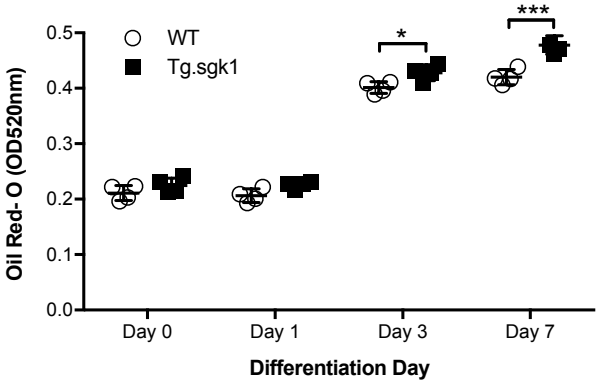

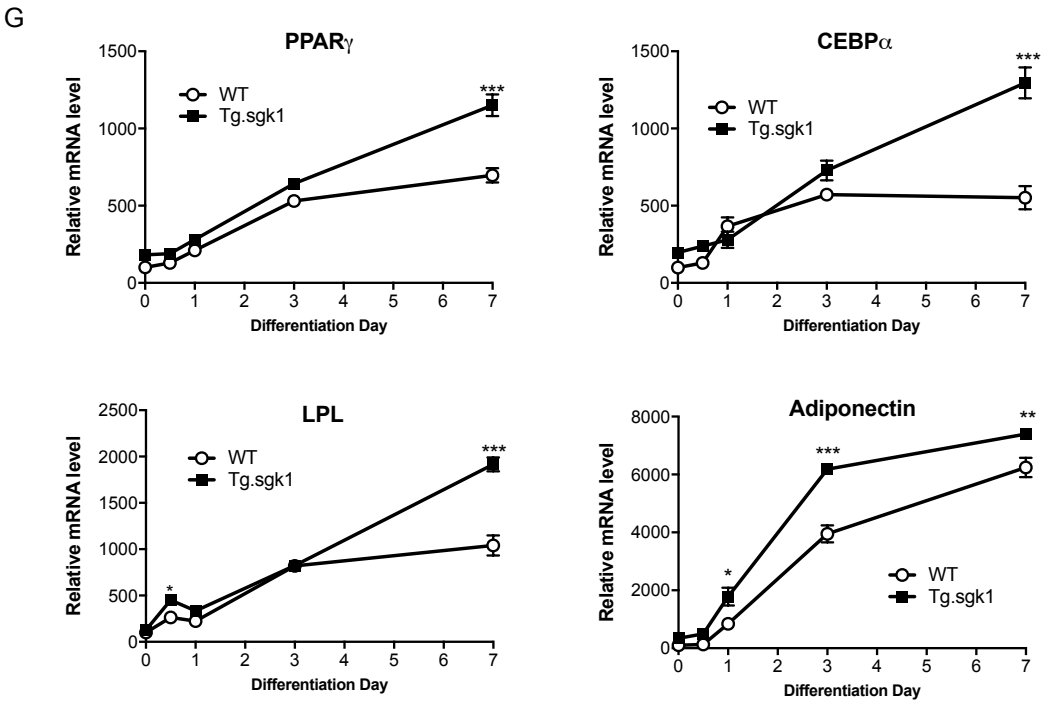

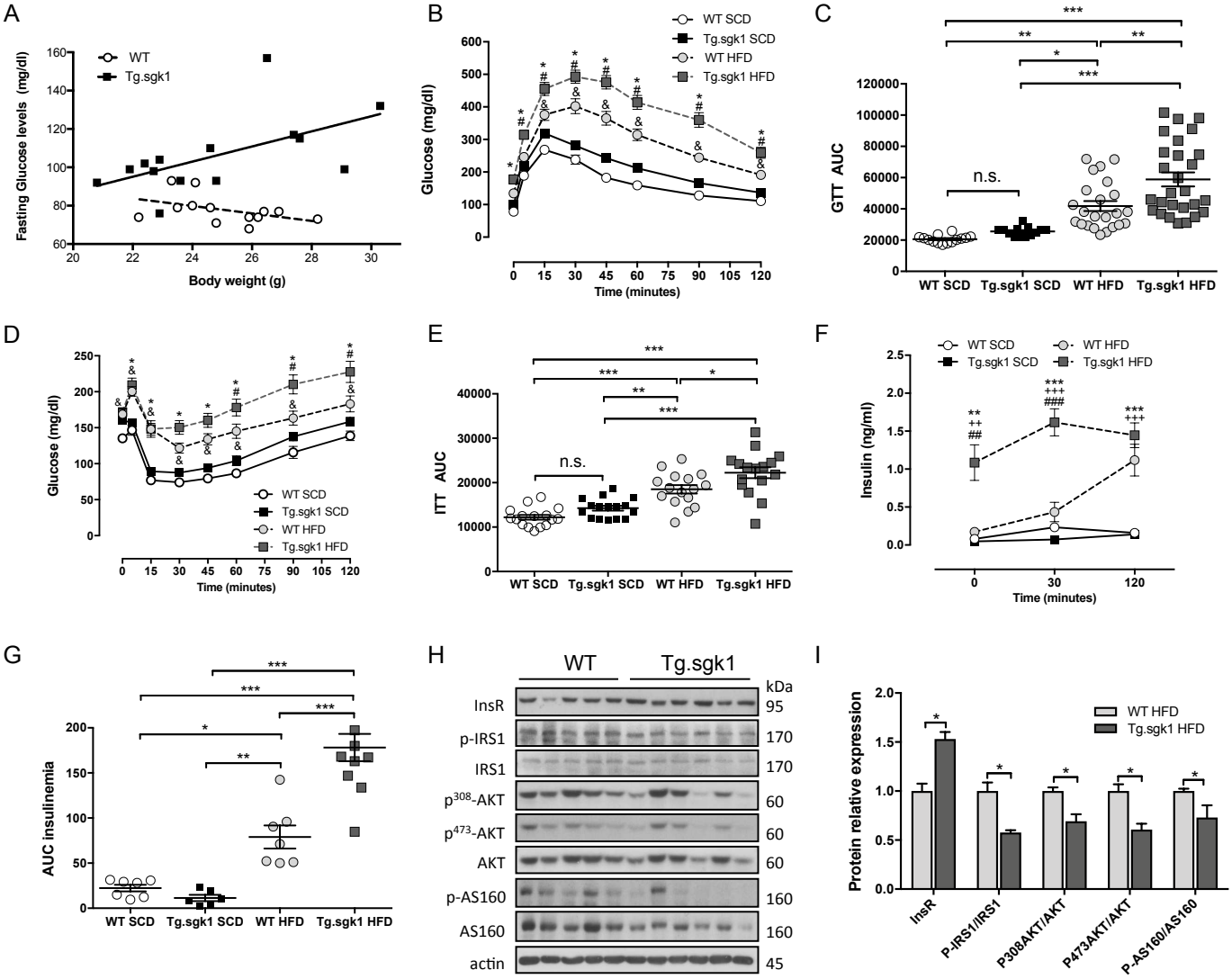

 Accepted Manuscript published as JOE-19-0275.R1. Accepted for publication: 10-Oct-2019

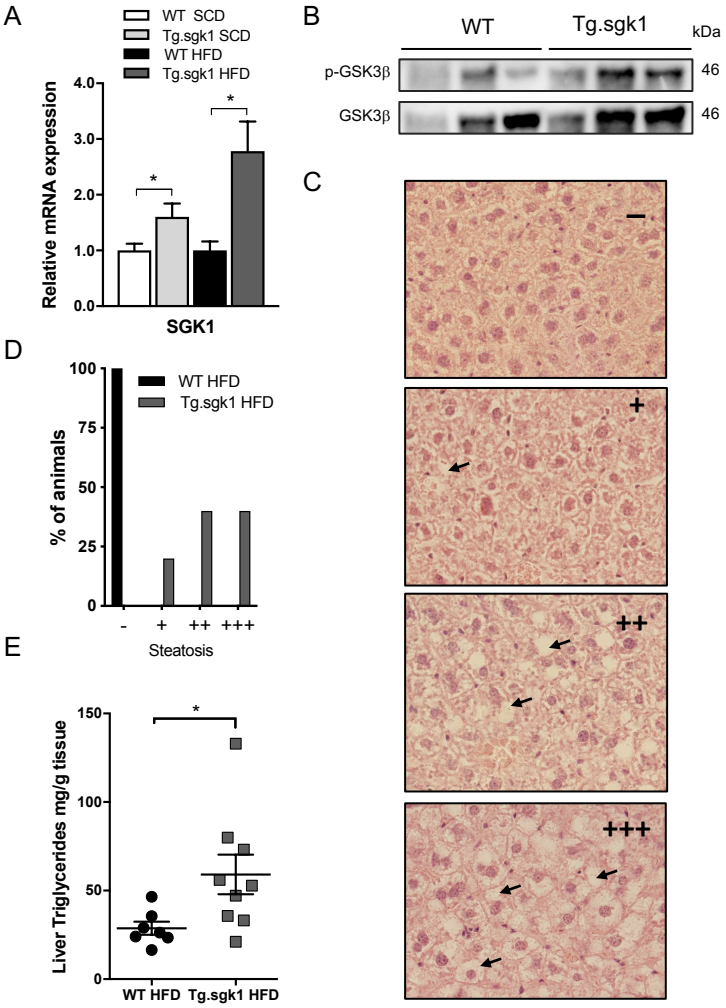

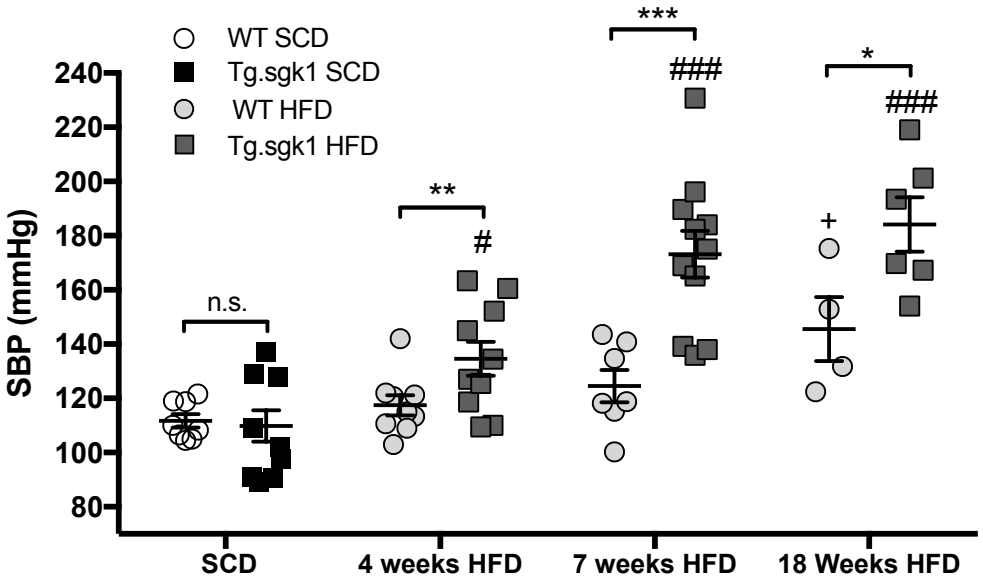

Accepted Manuscript published as JOE-19-0275.R1. Accepted for publication: 10-Oct-2019

Table 1. Primers used in this study

Gene	*Forward*	*Reverse*
Sgk1	CGGTTTCACTGCTCCCCTCAG	GCGATGAGAATCGCTACCATT
Il1	TGGACAAACACTATCTCAGCA	GAGTTTTGGTGTTTCTGGCA
Il6	TCTCTGGGAAATCGTGGAAA	CCAGGTAGCTATGGTACTCC
Tnfα	CCCCAAAGGGATGAGAAGTT	TCTTTGAGATCCATGCCGTT
Cd68	AAAGGCCGTTACTCTCCTG	TGTGGCATGAGAAATTGTGG
Mcp1	GTCACCAAGCTCAAGAGAGA	GTGGAAAAGGTAGTGGATGC
Glut4	ACACTGGTCCTAGCTGTATTCT	CCAGCCACGTTGCATTGTA
Cd36	GATGACGTGGCAAAGAACAG	TCCTCGGGGTCCTGAGTTAT
Pparγ	TTCACAAGAGCTGACCCAAT	AAGCCTGATGCTTTATCCCC
Cebpα	GACAAGAACAGCAACGAGTA	AGCTGGCGGAAGATGC
Lpl	GGAGGTGGACATCGGAGAAC	ACACTGCTGAGTCCTTTCCC
Adiponectin	TGCCGAAGATGACGTTACTA	TCTCACCCTTAGGACCAAGA

Table 2. Antibodies used in this study. RRID, research resource identifier.

Peptide or protein target	Antigen sequence	Name of Antibody	Manufacturer, or provider	Species raised in; monoclonal or polyclonal	Dilution used	RRID or Reference
Nedd4-2	Synthetic peptide surrounding E271 of human NEDD4-2	NEDD4L	Cell Signaling, catalog #4013	Rabbit polyclonal	1:1000	AB_1904063
p-Nedd4-2	Phospho-NEDD4-2 (S448)	Phospho-NEDD4L (Ser448)	Cell Signaling, catalog #8063	Rabbit polyclonal	1:1000	AB_10890702
GSK3-β	Synthetic peptide of human GSK-3β.	GSK-3beta (27C10)	Cell Signaling, catalog # 9315	Rabbit monoclonal	1:1000	AB_490890
pGSK3α/β	Synthetic phosphopeptide of human GSK3α	Phospho-GSK3α-β (S21/9)	Cell Signaling, catalog # 9331	Rabbit polyclonal	1:1000	AB_329830
Insulin Receptor	Recombinant cytoplasmic domain of human Insulin Receptor beta	Anti-Insulin Receptor β antibody C18C4	Abcam	Mouse monoclonal	1:500	AB_1209215
p-IRS1	Peptide containing human phosphorylated Y632 IRS-1	p-IRS-1 (Y632)	Santa Cruz Biotechnology	Rabbit polyclonal	1:1000	AB_669445
IRS1	Synthetic peptide conjugated to KLH, surrounding amino acids 634-638 of Human IRS1	Anti-IRS1 antibody	Abcam	Rabbit polyclonal	1:500	AB_11156316
p-AKT T308	Synthetic phosphopeptide around T308 of mouse Akt	Phospho-Akt (T308)	Cell Signaling, catalog #9275	Rabbit polyclonal	1:1000	AB_329828
p-AKT S473	Synthetic phosphopeptide around S473 of mouse Akt	Phospho-Akt (S473)	Cell Signaling, catalog #9271	Rabbit polyclonal	1:1000	AB_331591
AKT	COOH-terminus of mouse AKT	AKT	Cell Signaling, catalog #9272	Rabbit polyclonal	1:1000	AB_329827
p-AS160	Synthetic peptide corresponding to the sequence around T642 of human AS160	Phospho-AS160 (T642) Antibody	Cell Signaling, catalog #4288	Rabbit polyclonal	1:1000	AB_10545274
AS160	EAITFTARKHPFPNEVSVDFC	anti-TBC1D1	Dr. J. Loffing (University of Zurich);	Rabbit polyclonal	1:2000	Di Chiara et al. *Am J Physiol Renal Physiol*. 309:F779, 2015
ß-actin	NH2-terminus of human ß-actin	anti-ß-actin (8H10D10)	Cell Signaling, catalog #3700	Mouse monoclonal	1:10000	AB_2242334
Purified Ig fractions, rabbit serum		Amersham ECL Mouse IgG, HRP-Linked Whole Ab	GE Healthcare, catalog #NA931	Donkey polyclonal	1:20000	AB_772210
Purified Ig fractions, mouse serum		Amersham ECL Rabbit IgG, HRP-Linked Whole Ab	GE Healthcare, catalog #NA934	Sheep polyclonal	1:20000	AB_772206

Accepted Manuscript published as JOE-19-0275.R1. Accepted for publication: 10-Oct-2019

Table 3. Plasma biochemistry and glucose homeostasis indexes in animals fed standard chow diet (SCD) or after 6 weeks with high-fat diet (HFD). Results are expressed as average ± SE (n, number of animals; *p<0.05, **p<0.01, ***p<0.001; unpaired t tests between genotypes in SCD or HFD). BW, body weight; FFAs, free fatty acids; HOMA, homeostatic model assessment; QUICKI, quantitative insulin sensitivity check index; T-Cholesterol, Total cholesterol; HDL-C, high-density lipoprotein cholesterol; VLDL-C, very low-density lipoprotein cholesterol.

	SCD		*HFD*	
Variable (units)	*WT*	*Tg.sgk1*	*WT*	*Tg.sgk1*
Body weight (g)	25.49 ± 0.38; n=50	24.94 ± 0.48; n=56	31.51 ± 0.77; n=50	34.83 ± 0.76**; n=56
Lean tissue (g/BW)	0.41 ± 0.01; n=6	0.38 ± 0.01; n=6	0.58 ± 0.02; n=31	0.50 ± 0.01**; n=35
Fat tissue (g/BW)	0.24 ± 0.00; n=6	0.31 ± 0.02**; n=6	0.31 ± 0.02; n=31	0.44 ± 0.01***; n=35
Non-fasting insulin (ng/ml)	0.44 ± 0.07; n=8	0.48 ± 0.10; n=6	1.66 ± 0.15; n=6	5.51 ± 0.88**; n=6
Fasting insulin (ng/ml)	0.08 ± 0.04; n=7	0.04 ± 0.03; n=7	0.17 ± 0.03; n=7	1.09 ± 0.23**; n=11
Fasting glucose (mg/dl)	97.6 ± 4.7; n=7	129.0 ± 7.9**; n=11	158.0 ± 4.8; n=7	200.2 ± 14.4* n=10
HOMA-IR	0.4 ± 0.2; n=7	0.3 ± 0.2; n=7	1.7 ± 0.3; n=7	13.2 ± 2.9**; n=11
QUICKI	0.55 ± 0.13; n=7	0.82 ± 0.16; n=7	0.32 ± 0.01; n=7	0.26 ± 0.00**; n=12
T-Cholesterol (mg/ml)	62.86 ± 5.9; n=6	68.14 ± 10.25; n=6	110.8 ± 5.6; n=6	108.6 ± 2.9; n=6
HDL-C (mg/ml)	59.6 ± 2.3; n=6	45.7 ± 4.0; n=6	114.5 ± 3.6; n=6	91.4 ± 7.7***; n=6
VLDL-C (mg/ml)	2.5 ± 0.6; n=6	5.7 ± 1.0; n=6	3.1 ± 1.0; n=6	4.2 ± 0.5; n=6
Triglycerides (mg/dl)	52.3 ± 8.0; n=6	84.8 ± 12.9; n=6	82.8 ± 9.8; n=6	123.7 ± 11.7*; n=6
FFAs (mmol/dl)	7.8 ± 1.0; n=6	8.8 ± 0.4; n=6	7.0 ± 0.8; n=6	8.0 ± 0.5; n=6